

EXPERIMENT OF AUTONOMOUS ORBIT CONTROL ON THE DEMETER SATELLITE

Alain LAMY, Marie-Claire CHARMEAU, Denis LAURICHESSE, Michel GRONDIN, Régis BERTRAND

*Centre National d'Etudes Spatiales (CNES)
18 avenue Edouard Belin, 31401 Toulouse Cedex 9, France
E-mail: Alain.Lamy@cnes.fr*

ABSTRACT

An in-flight demonstration of Autonomous Orbit Control (AOC) will be carried out in 2004/2005 on the French micro-satellite DEMETER. The experiment aims at computing and performing station keeping maneuvers on board and autonomously. It is based on a TOPSTAR 3000 GPS receiver including the "DIOGENE" orbital navigator. In order to limit the impacts on the satellite platform, the maneuver computation software is installed in the GPS receiver, whereas the effective velocity and attitude maneuvering commands are generated by a dedicated piece of software installed in the payload management unit.

This paper will first introduce the experiment and its context. Some simulation results will be shown in order to illustrate the expected long-term station keeping performance. Finally, newly obtained in-flight results of the navigation performance and of the maneuver computation software behavior will be presented.

1. EXPERIMENT CONTEXT

CNES has for long been involved in activities related to on-board navigation, as proved by the successful in-flight results obtained by the orbital navigators DIODE on SPOT4 and DIOGENE on HETE2 [3]. A research and technology program has been led by CNES since 1998 in order to demonstrate that on-board autonomy can be a good option for future missions. Part of this program is an in-flight demonstration of autonomous orbit control in 2004/2005 on the DEMETER satellite.

DEMETER was successfully put in orbit on June 29th 2004 by a DNEPR launcher. The experiment implementation is still at an early stage, yet some first in-flight results have been obtained. Before showing them along with some other simulation results, the experiment and its context will be presented in details.

1.1 Autonomy issues

Increasing the autonomy of satellites often inspires fears, since autonomy is generally seen as an additional unnecessary risk. For this reason, in-orbit experiments are needed to really demonstrate what exactly these new

techniques are up to. With the advances in on-board processing capabilities and the existence now of off-the-shelf orbital navigators able to provide accurate and real-time satellite position and velocity, it makes sense to perform both orbit determination and maneuver computation on board.

One advantage of autonomy applied to orbit control lies in the possibility to perform more frequent, hence smaller maneuvers. This decreases the impact of possible maneuver execution errors. It also reduces the need for complex prediction models in the calculations so that the complexity of the algorithms should, in principle at least, decrease too.

1.2 DEMETER: an opportunity for a demonstration of autonomous orbit control

DEMETER is the first micro-satellite from the new product line designed by CNES to provide scientists with a platform suitable to fly scientific experiments within a short time. It is endowed with a twofold scientific and technological mission. The objective of the scientific mission is the detection of signs of tectonic activity, i.e. earthquakes. DEMETER's orbit is nearly circular with an altitude close to 700 km. It is also almost sun-synchronous.

Although DEMETER's scientific mission does not require orbit maintenance, the satellite is equipped with a propulsion system for qualification purposes. This particularity makes DEMETER an ideal opportunity for a test of autonomous orbit control. It was then logically decided to have such an experiment included into DEMETER's technological mission. This meant adding to the payload means to compute the orbit in real time as well as software able to compute the needed maneuvers and to generate and send commands to the platform.

1.3 Constraints imposed to the experiment

DEMETER has not been designed for autonomy, so that the design of the AOC experiment had to cope with a good number of specific constraints either related to the

satellite platform, the scientific mission or the ground segment.

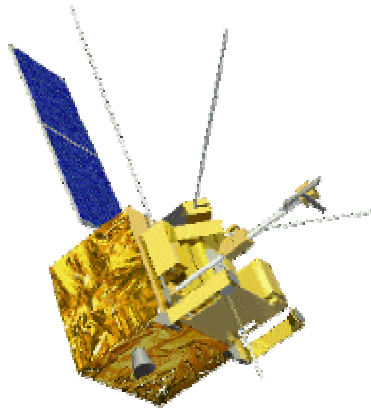


Fig. 1: DEMETER

Constraints coming from the satellite design. The propulsion system of DEMETER is composed of four hydrazine thrusters located on the face opposite the Earth. Consequently, performing tangential orbit corrections implies to rotate the satellite 90 degrees. This is achieved in the so-called “orbit control mode” in which the sensors are gyrometers and the actuators are reaction wheels. The commands to the platform have then to handle the change from nominal to orbit control mode, the attitude profile during the rotation, the activation of the thrusters, the attitude profile back to nominal attitude and the return to nominal mode. This sequence must not last too long because of the gyrometers’ drift uncertainty. Due to the limited reaction wheel capacity, about a quarter of an orbit (25mn) is needed for a 90 degree rotation. It is then not possible to perform two burns on the same orbit. In consequence, each maneuver will also result in a slight eccentricity change.

Constraints coming from the scientific mission. The scientific instruments cannot be used when the satellite attitude is not the nominal (geocentric) one. A trade-off with the scientific team led to limit the number of maneuvers by defining slots in which orbit corrections are only to occur. Two slots per week are defined. Each slot is 1.5 orbit long, including time for attitude change, which enables corrections at any desired position. In addition, specific periods entirely dedicated to the AOC experiment are also planned. During these 1-month periods, the maneuver frequency can be up to 2 per day.

Constraints coming from the ground segment. The ground control center has its own independent means to determine the orbit in order to point the ground antennas at the satellite. Moreover, it is not aware of the exact amplitude of the maneuvers computed on board. If the satellite trajectory is too much changed by an autonomous orbit correction, the satellite might be lost. This led to limit the amplitude of the maneuvers that can

be autonomously performed on board. The resulting maximum velocity increment allowed is 11mm/s. It corresponds roughly to a semi-major axis change of 20m.

Technological constraints. Besides the relatively high value of the minimum velocity increment ($\approx 1\text{mm/s}$), the maneuver computation algorithms have to cope with possibly high execution errors, since the expected maneuver amplitudes are close to the smallest ones enabled by the propulsion system.

Last minute constraints. Additional constraints came late in the development process due to the unusual sensitivity of the scientific instruments to electromagnetic disturbances. This led to restrain the movement of the solar array, thus impacting the power budget. Consequently, the GPS receiver had to stay in stand-by mode most of the time.

In the nominal (routine) scenario, the GPS receiver is operational for only about 10mn above the poles and during the maneuver slots (1.5 orbit long, twice a week). These conditions are particularly stringent, as the orbit control algorithms will have very few (moreover of lesser quality) navigation inputs. This obviously impacts the performance, expected to be not as good as initially planned. But during the “AOC dedicated month” the receiver will be operating continuously, which will give a better idea of the performance that can be reached on DEMETER.

2. THE ORBIT CONTROL EXPERIMENT

2.1 On-board architecture

The architecture chosen for this experiment is quite specific, due to the location in the payload rather than in the platform.

The real-time orbit is obtained by an Alcatel TOPSTAR 3000 GPS receiver [2]. The TOPSTAR 3000 is a single frequency (L1) receiver that includes the “DIOGENE” orbital navigator [1] [4].

The specific software in charge of the maneuver computation has been installed in the GPS receiver for convenience. It is fed with navigation data through a dedicated interface, and uses these to compute the needed velocity increments. It also computes many other intermediate results that are supplied to the ground by the receiver telemetry, extended for the need of the experiment.

The payload monitoring unit (PMU) is in charge of the control of the GPS receiver, of the extraction of the maneuver from the receiver telemetry and of its translation into commands that can be understood by the satellite platform processing unit.

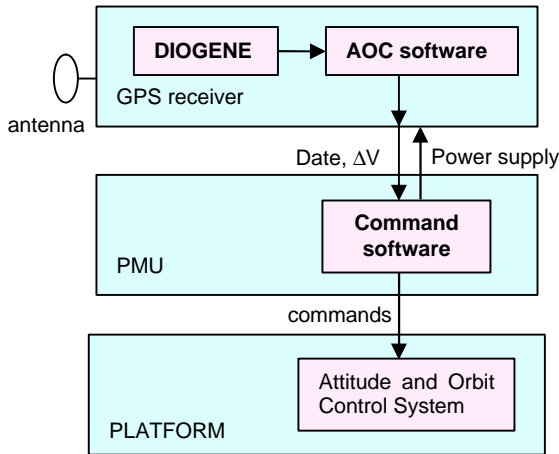


Fig. 2: On-board architecture

The GPS receiver provides the maneuver computation software with two data sets every 30 seconds. These data consist of the position and velocity relative to WGS84, the associated time (in the GPS time scale), and additional confidence and validity indicators. One of the data set contains the orbit parameters as determined by DIOGENE, the other contains the solution given by the instantaneous least squares fit. It will then be possible to measure the performance of the autonomous station keeping algorithms, when using either of these two data sources.

2.2 Station keeping concerns and objectives

One of the major concerns was to design demonstrative enough an experiment without adding unnecessary complexity to the algorithms. It was then decided to only perform in-plane maneuvers, approximately along the velocity, whether in the same direction or not.

For the typical implementation, the choice was classically made to control the longitudes of the ground tracks at the equator while keeping the perigee frozen. Other backup options also exist: control of the date at the equator, or of the mean semi major axis; these options will not be mentioned any further in this paper.

The reference longitudes at successive ascending nodes are expressed by:

$$L(n) = L_0 + D * (n - n_0) + \delta$$

where n is the node number (counted from some reference node n_0), L_0 is the longitude at node n_0 , D is the constant mean difference of longitude between two consecutive ascending nodes, and δ is a correction term explained later. In practice, D is defined as a function of the 3 integer phasing parameters N, P, Q by:

$$D = \frac{-2\pi Q}{N * Q + P}$$

The tesseral terms of the Earth potential are known to deflect the ground tracks so that the “true” longitudes at the ascending nodes are not in fact evenly distributed.

The distance between the true longitudes and the evenly distributed ones is given by an expansion of the form:

$$\delta(L) = \delta_0 + \sum_{k \geq 1} a_k \cos(kL) + b_k \sin(kL)$$

where L is the longitude of ascending node, and δ_0, a_k, b_k are constant parameters defined up to the desired expansion order. The correction terms are not highly dependent on the actual orbit and may consequently be computed and uploaded once.

2.3 DV computation principles

Maneuver computation is essentially simple. It is based on the estimation of evolution (i.e. prediction) models for a few relevant parameters. These parameters are primarily the distance to the reference ground tracks DL (fit to a 2nd order polynomial) and the mean eccentricity vector.

Depending on the predicted evolution of DL , a maneuver may be required or not. If so, its approximate date is given by the next maneuver slot and its precise position is computed using the mean eccentricity vector. The calculation of the ΔV amplitude is more complex. It basically aims at keeping DL as close to 0 as possible, while taking account of the impacts of erroneous model estimation or maneuver execution errors.

The main algorithm tasks are summarized in fig. 3. But this too simple schematic hides in fact most computation features. For more explanations on the algorithms: data selection, two-stage model determination by Kalman filters, model estimation tuning, maneuver computation and control strategies..., refer to [5].

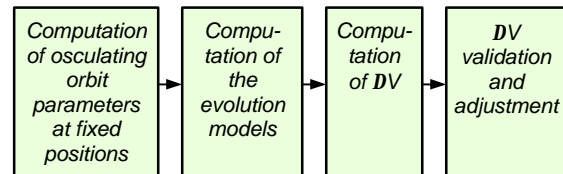


Fig. 3: Main maneuver computation tasks

2.4 A progressive implementation

Three distinct phases will occur in sequence:

- Passive, routine phase

During this phase, all the computations tasks are performed normally in accordance with the routine scenario (i.e. 2 maneuvers per week at the most, receiver operating above the poles and within the maneuver slots), but the final commands are not sent to the platform. This phase primarily exists because the

propulsion system must not be activated for the first 5 months in orbit. This period will be turned to good account for the commissioning of the orbit control algorithms.

- Active, routine phase

This phase is quite similar to that described above, except for the maneuver commands that are sent to the platform for execution. No maneuver will be executed before November 2004.

- Continuous phase

A third phase planned later on will enable up to 2 maneuvers per day owing to the interruption of the scientific mission during this period.

3. VALIDATION PROCESS

3.1 From simulation to real time validation

The main validation means used are:

- a simulator (1) that can run the flight AOC algorithms,
- an ERC32 test bed on which the flight software was validated before being integrated into the GPS receiver,
- a GPS constellation test bed (2) including an engineering model of the GPS receiver,
- the satellite flight model connected to the GPS constellation simulator.

All the software specifically developed for the experiment has been validated by both simulation and real-time tests. Simulation tests were used to check the behavior of the AOC algorithms and to assess their performance. Real-time tests were used to validate the flight code and to evaluate the receiver performance in operational conditions.

The simulator (1) is shown on fig 4.

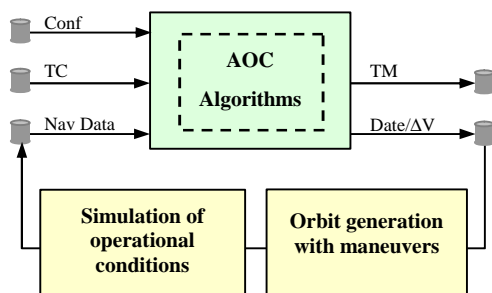


Fig. 4: AOC simulator architecture

The AOC algorithms are embedded in a specific program named “AOC monitor” that calls the AOC interfaces the exact way the receiver does on board. The “AOC monitor” is connected to an orbit propagator able to take the orbit control maneuvers into account (including possible execution errors). The 3rd element

simulates the operational conditions: activation periods of the receiver as well as orbit determination errors.

The GPS test-bed (2) is composed of an engineering model of the TOPSTAR 3000 receiver containing the flight software, a simulator of the GPS constellation that computes all the signals emitted by the GPS satellites, and a specific module that converts these computed signals into real signals to be emitted towards the receiver antenna. Commands are sent to the receiver to set it in operational or stand-by mode as needed.

The GPS test-bed has been used in various circumstances: for the tuning of the receiver and DIOGENE behaviors, in conjunction with the AOC simulator (by injecting the observed navigation errors into the long-term AOC simulation tests), or in connection with the satellite flight model before launch. The test-bed is still being used in order to test optimized command sequences before sending them to the satellite.

3.2 Long-term AOC simulation sample result

This part aims at illustrating the routine performance of the orbit control algorithms and in conditions close to those expected in orbit.

The main hypotheses used are the following:

- Orbit: altitude ≈ 700 km (phasing parameters = 14+17/30), local hour of descending node: 10h30, initial eccentricity nearly frozen.
- Satellite: mass = 110 kg, area (exposed to the atmosphere) = 1 m².
- Simulation epoch: from mid 2004 to end of 2005.
- Orbit propagation model: all major forces considered. Shifted “true” solar activity used to compute the effect of drag.
- Navigation: the GPS receiver supplies the AOC algorithms with valid navigation data at the poles only (measurement intervals from 2.5 to 5.5mn randomly distributed). Their accuracy is assumed to be given by: 3D position error: 80m (99.7%), 3D velocity error: 0.3m/s (99.7%).
- Maneuver execution: relative $|\Delta V|$ error: 100% (3σ).

Figure 5 illustrates the performance obtained: around 300m at the equator on Earth surface most of the time. The peak visible near Sept 14th 2004 (●) is typical of the effect of an increase of solar activity combined with the execution of several too small maneuvers consecutively. Both effects prevent the controlled parameter to come back to 0 quickly enough. Some tuning parameters exist in order to try to manage this kind of undesirable behavior.

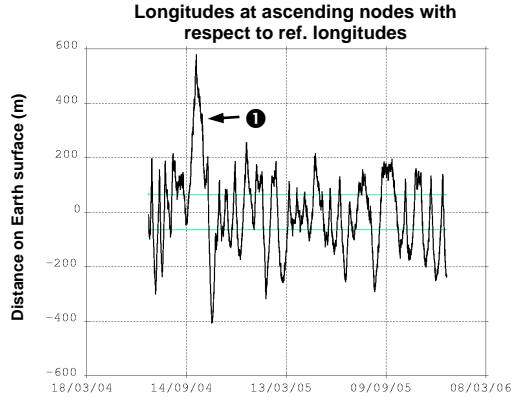


Fig. 5: Orbit control estimated performance

NB: The performance is limited by the maximum maneuver frequency and by maneuver errors. The performance achievable without these constrains would be far better.

Figure 6 shows the corresponding velocity increments. Clearly visible is the higher density of maneuvers at the beginning of the simulation due to a stronger solar activity. “Negative” maneuvers are performed from time to time, mainly to make up for excessive maneuver execution errors.

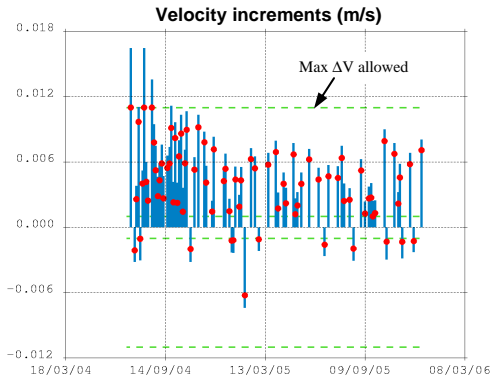


Fig. 6: Computed AOC velocity increments

4. FIRST IN-FLIGHT RESULTS

DEMETER was launched on June 29th 2004. The first month in orbit was devoted to the commissioning of the on-board equipment, and during this month the receiver was activated 3 times for limited periods. The (passive) routine mode was expected to begin in early August, but unpredicted events unfortunately forced the receiver to be switched off several times. Nonetheless, some promising results have still been obtained.

4.1 First activation of the GPS receiver (July 2004)

The receiver was activated for the first time on July 13th 2004. It ran continuously for about 12 hours as expected.

The number of tracked satellites is plotted on fig. 7 as a function of time. This number is in the range 2-8 depending on the geometry of the GPS constellation as seen from the antenna (oriented towards the normal of the orbit plane). Since it may occasionally be below 4, no position fix is guaranteed at all times.

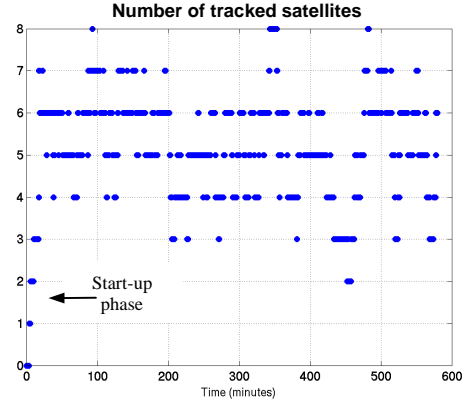


Fig. 7: Number of tracked GPS satellites

Figure 8 shows the real-time orbits obtained during the same period. Both the orbit from DIOGENE (black thick curve) and the instantaneous position/velocity computed directly by the receiver (discontinuous light curve) are compared to a reference orbit recomputed off-line using the CNES ZOOM software. The reference orbit accuracy is estimated at meter level thanks to code / carrier phase processing that eliminates the effects of the ionosphere on the measurements.

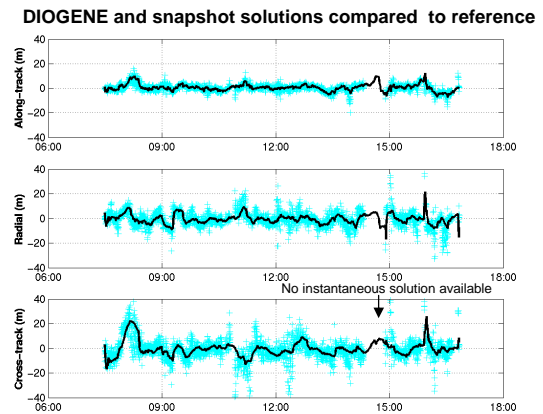


Fig. 8: DIOGENE and snapshot performance

The solution supplied by DIOGENE is clearly of better quality (smoother, available 100% of the time) owing to the accurate propagation model used. Yet, some improvements could probably be obtained by a better choice of tuning parameters (so that more confidence be given in the orbital model).

	Cross-track	Radial	Along-track
Mean (m)	-0.5	-0.6	0.5
Std. dev. (m)	5.9	3.7	2.9

Table 1: DIOGENE accuracy

The position accuracy is synthesized in table 1. The higher value for the cross track component probably results from the orientation of the antenna.

4.2 Routine mode (August 2004)

From August 15th to August 22nd 2004, the receiver was activated according to the routine scenario.

The behavior of the on-board AOC algorithms proved nominal, as could be checked in the telemetry. The software reacted correctly to the limited number of commands sent from the ground.

But it was too soon to have maneuvers computed on board. Instead, the telemetry coming from the receiver (including all the data sent to the AOC algorithms) has been used off-line to run the AOC software with real data as inputs.

Figure 9 shows the true orbit positions ($w+v$) corresponding to the DIOGENE data processed by the AOC algorithms. One clearly sees the maneuver slots every 3 and 4 days alternately as well as the small orbit portions above the poles during which the receiver yields valid data.

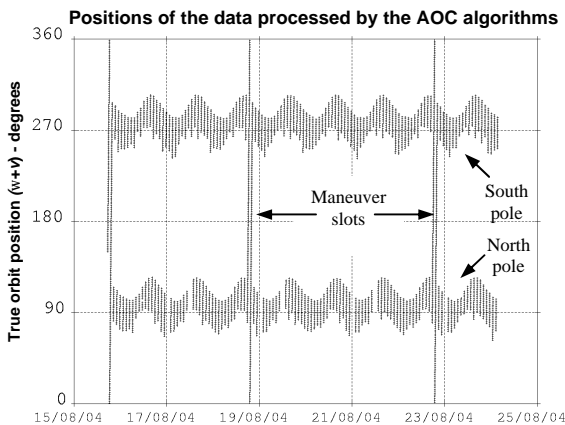


Fig 9: GPS receiver activation periods

Figure 10 illustrates the processing performed by the OAC algorithms when fed with the DIOGENE data. The estimated model for the controlled parameter (distance to the reference longitudes) is plotted as it is estimated.

Adequate tuning parameters have been used, and in particular some periodic terms (2, 1, 2/3 days) have been filtered in order to increase the final accuracy. The same results could have been obtained on board if the chosen tuning parameters had been uploaded.

It can be concluded that the model seems both accurate and stable enough (after a certain convergence time) to enable maneuver computation. The accuracy obtained also appears to be consistent with the simulation results shown in paragraph 3.2.

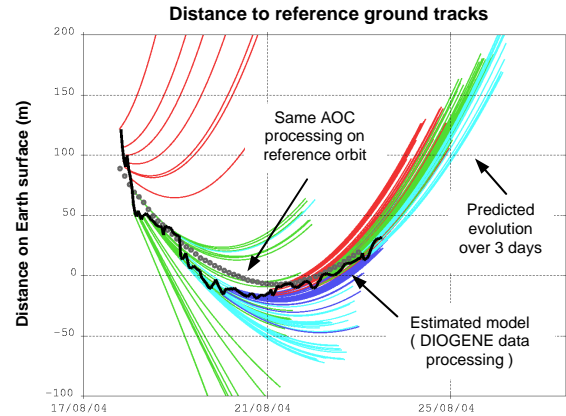


Fig 10: AOC model estimation

5. CONCLUSION AND PERSPECTIVES

The main features of the orbit control experiment on DEMETER have been presented: design constraints, operational characteristics, validation process and expected performance.

The first in-flight results obtained, some of which were shown in this paper, look promising.

The next step will consist in having all the calculations performed on board, which should happen very soon. The months to come will then be devoted to result checking and finer tuning of the receiver behavior and of the AOC algorithms. This period will also allow for some useful operational practice.

Once this in-orbit validation phase is over, the experiment should be in a state suitable for the execution of the first autonomous maneuver by the end of 2004.

References

1. C. Mehlen, D. Laurichesse *Improving GPS navigation with orbital filter*, Proceedings of 4th ESA conference on spacecraft guidance navigation and control systems, october 1999.
2. JL Gerner, JL. Issler, D. Laurichesse, C. Mehlen and N. Wilhelm (2000), *TOPSTAR 3000, An enhanced GPS receiver for space application*, ESA Bulletin, Oct. 2000.
3. JP. Berthias et al (CNES), *Lessons learned from the use of a GPS receiver in less than optimal conditions*, 16th ISSFD, Pasadena, 3-7 December 2001.
4. C. Mehlen (ALCATEL), D. Laurichesse (CNES), *Real-time GEO orbit determination using TOPSTAR 3000 GPS receiver*. Proceedings of ION GPS international meeting, september 2000.
5. A. Lamy and MC. Charmeau (CNES), *Performance of the autonomous orbit control of the DEMETER satellite*, AIAA-2002-4906.